Discretization of the Lotka–Volterra System and Asymptotic Focal and Prefocal Sets

Jean-Pierre Françoise, Danièle Fournier-Prunaret

DISCRETIZATION OF THE LOTKA-VOLTERRA SYSTEM AND ASYMPTOTIC FOCAL AND PREFOCAL SETS

J.P. FRANÇOISE AND D. FOURNIER-PRUNARET

ABSTRACT. We revisit the Kahan-Hirota-Kimura discretization of a quadratic vector field. The corresponding discrete system is generated by successive iterations of a birational map F_h. We include a proof of a formula for the Jacobian of this map. In the following, we essentially focus on the case of the Lotka-Volterra system. We discuss the notion of focal points and prefocal lines of the map F_h and of its inverse F_h^{-1}. We show that the map F_h is the product of two involutions. The nature of the fixed points of F_h is studied. We introduce the notion of asymptotic focal and prefocal sets. We further provide a proof of the theorem of Sanz-Serna. We show that the mapping F_h is integrable for $h = 1$ and that it preserves a pencil of conics (generic hyperbolas). To conclude, we provide several numerical simulations for $0 < h < 1$.

Keywords: Kahan-Hirota-Kimura discretization, quadratic planar vector fields, birational mappings, discrete Lotka-Volterra system, focal point, knot point, prefocal set, asymptotic focal set, asymptotic prefocal set, theorem of Sanz-Serna, numerical simulations

1. INTRODUCTION

The Kahan discretization was introduced in the unpublished lecture notes of a AMS congress organized at the Fields Institute in 1993 ([Kahan(1993)]). The next appearance of this discretization was in two articles of Hirota and Kimura in 2000 ([Hirota & Kimura(2000), Kimura & Hirota(2000)]) where it was shown that in several cases the method preserves integrability. According to a proposal of T. Ratiu, discretizations of KHK type should be considered for numerous integrable systems ([Ratiu(2006)]). In this paper, we mainly focus on Quadratic Planar Vector Fields and more precisely on the KHK discretization of the Lotka-Volterra system.

$$\dot{z} = f(z) = Q(z) + B(z) + c \qquad z = (x, y) \in \mathbb{R}^2. \tag{1}$$

Each component of $Q : \mathbb{R}^2 \to \mathbb{R}^2$ is a quadratic form, while $B \in Gl(2,\mathbb{R})$, the group of invertible 2x2 matrices with real entries under matrix multiplication, and $c \in \mathbb{R}^2$.

The Kahan-Hirota-Kimura (KHK) discretization of the Quadratic Planar Vector Fields is the mapping $z \mapsto z'$ defined as:

$$\begin{aligned} \frac{z'-z}{h} &= Q_1(z,z') + \frac{1}{2}B(z+z') + c, \\ z = (x,y) \in \mathbb{R}^2, z' &= (x',y') \in \mathbb{R}^2 \end{aligned} \tag{2}$$

where $Q_1(z,z') = \frac{1}{2}[Q(z+z') - Q(z) - Q(z')]$ is the symmetric bilinear form corresponding to the quadratic form Q.

In the case of quadratic vector field, this mapping can be identified with the (implicit) Runge-Kutta discretization ([Celledoni *et al.*(2013)]) :

$$\frac{z'-z}{h} = -\frac{1}{2}f(z) + 2f(\frac{z+z'}{2}) - \frac{1}{2}f(z'), \tag{3}$$

Expanding the Taylor series about z shows that ([Celledoni *et al.*(2013)]) :

$$\frac{z'-z}{h} = f(z) + \frac{1}{2}Df(z)(z'-z). \tag{4}$$

where $Df(z)$ is the Jacobian matrix of f at z. This yields an explicit KHK rational map:

$$z' = F_h(z) = z + h(I - \frac{h}{2}Df(z))^{-1}f(z), \tag{5}$$

Another remarkable point is that:

$$F_h^{-1}(z) = F_{-h}(z), \tag{6}$$

and thus, in particular, the KHK-map is birational. Further references on the subject include ([Celledoni *et al.*(2015), Celledoni *et al.*(2014), Celledoni *et al.*(2013), Duistermaat(2010), Francoise & Ragnisco(1999), Gálvez-Carrillo & Mañosa(2015), Van der Kamp *et al.(2021)*, Quispel *et al.(1988)*, Quispel *et al.(1989)*, Petrera *et al.(2019)*]).

2. The discrete Lotka-Volterra system, focal points, prefocal lines and asymptotic focal and prefocal sets

2.1. **A key formula for the Jacobian.**

Theorem 1. *Consider a KHK-map of a quadratic vector field in any dimension n :*

$$F_h : z = (x_1, ...x_n) \mapsto z' = (x'_1, ...x'_n). \tag{7}$$

Set $\Delta = \Delta(z, h) = \mathrm{Det}(I - \frac{h}{2}Df(z))$ *and denote* $\Delta' := \Delta(z', -h)$*; the following formula can be shown:*

$$\frac{dx_1 \wedge ... \wedge x_n}{\Delta} = \frac{dx'_1 \wedge ... \wedge x'_n}{\Delta'}. \tag{8}$$

Be careful that this relation cannot be interpreted as the conservation of a volume.

Proof. Denote $A = \frac{\partial z'}{\partial z}$ the Jacobian matrix of the coordinates z' relatively to z.

From the formula (3), we deduce

$$A - I = -\frac{h}{2}Df(z) + \frac{h}{2}2Df(\frac{z+z'}{2})(I + A) - \frac{h}{2}Df(z')A. \tag{9}$$

Using the fact that $Df()$ is linear, this yields

$$A = I - \frac{h}{2}Df(z) + \frac{h}{2}(Df(z) + Df(z'))(I + A) - \frac{h}{2}Df(z')A, \tag{10}$$

which displays:

$$(I - \frac{h}{2}Df(z))A = (I + \frac{h}{2}Df(z')), \tag{11}$$

this implies:

$$\Delta \mathrm{Det}A = \Delta'. \tag{12}$$

□

2.2. **The discrete Lotka-Volterra system.** After some scaling, the famous Lotka-Volterra system modeling the interaction of predator with prey can be written as

$$\begin{aligned} \dot{x} &= x(1-y) \\ \dot{y} &= y(x-1). \end{aligned} \tag{13}$$

This system is not Hamiltonian for the usual symplectic form but it is "generalized Darboux" integrable with $H = xye^{-(x+y)}$.

In order to avoid the appearance of various powers of 2, we change $h/2$ into h (cf. [Petrera *et al.(2009)*]). The KHK discretization yields to:

$$\begin{aligned} x' - x &= h[(x'+x) - (x'y + xy')] \\ y' - y &= h[(x'y + xy') - (y'+y)], \end{aligned} \tag{14}$$

and this displays:

$$\Delta := \Delta(x, y, h) = 1 - h^2 - h(1-h)x + h(1+h)y, \tag{15}$$

$$\begin{aligned} x' &= \frac{x}{\Delta}[(1+h)^2 - h(1+h)x - h(1-h)y] = \frac{xN_1(x,y)}{\Delta(x,y)} \\ y' &= \frac{y}{\Delta}[(1-h)^2 + h(1+h)x + h(1-h)y] = \frac{yN_2(x,y)}{\Delta(x,y)}. \end{aligned} \tag{16}$$

A first study of this map has been introduced in [Francoise & Fournier-Prunaret(2023)], where the model has been given, as well as some preliminary simulations, but the role of focal points and prefocal lines was not considered. In this paper, we study the properties of the map (16) by introducing the focal points and prefocal lines, that are specific to maps with denominators.

It should be noted that this KHK map leaves invariant both $x = 0$ and $y = 0$ (for $h \neq 1$), that are denoted :

$$\begin{aligned} D_0 &= \{(x, y) \mid y = 0\} \\ D_0' &= \{(x, y) \mid x = 0\} \end{aligned} \tag{17}$$

At this point, we add another important property which relates F_h and its inverse. Let $\sigma : (x, y) \mapsto (y, x)$ be the symmetry which exchanges the two canonical coordinates.

Proposition 2. *The inverse F_h^{-1} is conjugated to F_h through the symmetry σ:*

$$F_h^{-1} = \sigma(F_h(\sigma^{-1})). \tag{18}$$

If we denote $s_h = F_h \circ \sigma$, then s_h is an involution ; hence F_h is the product of two involutions :

$$F_h = s_h \circ \sigma. \tag{19}$$

The proof is quite immediate and is left to the reader.

2.3. **Focal points and prefocal lines.** Denote the three lines:

$$\begin{aligned} D &= \{(x,y) \mid \Delta(x,y) = 0\} \\ D_1 &= \{(x,y) \mid N_1(x,y) = 0\} \\ D_2 &= \{(x,y) \mid N_2(x,y) = 0\}. \end{aligned} \tag{20}$$

The straight lines D, D_1 and D_2 respectively correspond to the cancellation of the denominator and the numerators of x' and y' in (16). Let us define the points $B = (1 + \frac{1}{h}, 0)$ and $C = (0, 1 - \frac{1}{h})$, then

$$\begin{aligned} B &= D \cap D_1 \cap D_0 \\ C &= D \cap D_2 \cap D_0'. \end{aligned} \tag{21}$$

B and C are candidates as focal points in the sense of Bischi-Gardini-Mira [Bischi *et al.*(1999), Bischi *et al.*(2003), Bischi *et al.*(2005), Bischi *et al.*(2011), Gardini *et al.(1999)*, Gardini *et al.(2000)*, Tramontana(2016)]. The authors were mainly interested in the case where the mapping is noninvertible but the tools they introduced are also useful to understand the dynamics when the mapping is birational and invertible. Moreover, our case is different from those previously studied because the points B and C both cancel numerator and denominator of both components of the map F_h.

The formula $F_h^{-1}(x,y) = F_{-h}(x,y)$ allows to easily compute the inverse of F_h by changing h into $-h$. This defines three linear forms so that:

$$\begin{aligned} N_1'(x,y) &= (1-h)^2 + h(1-h)x + h(1+h)y \\ N_2'(x,y) &= (1+h)^2 - h(1-h)x - h(1+h)y \\ \Delta'(x,y) &= 1 - h^2 + h(1+h)x - h(1-h)y, \end{aligned} \tag{22}$$

and the application F_{-h}:

$$
\begin{aligned}
x' &= \frac{x}{\Delta'}[(1-h)^2 + h(1-h)x + h(1+h)y] = \frac{xN_1'(x,y)}{\Delta'(x,y)} \\
y' &= \frac{y}{\Delta'}[(1+h)^2 - h(1-h)x - h(1+h)y] = \frac{yN_2'(x,y)}{\Delta'(x,y)}.
\end{aligned} \tag{23}
$$

Denote

$$
\begin{aligned}
D' &= \{(x,y) \mid \Delta'(x,y) = 0\} \\
D_1' &= \{(x,y) \mid N_1'(x,y) = 0\} \\
D_2' &= \{(x,y) \mid N_2'(x,y) = 0\}.
\end{aligned} \tag{24}
$$

Let us define $B' = (1 - \frac{1}{h}, 0)$ and $C' = (0, 1 + \frac{1}{h})$, then

$$
\begin{aligned}
B' &= D' \cap D_1' \cap D_0 \\
C' &= D' \cap D_2' \cap D_0'.
\end{aligned} \tag{25}
$$

B' and C' may also be focal points for F_h^{-1}.

Let us recall that a point Q is a focal point ([Bischi *et al.*(1999)]) if at least one component of the map takes the form $0/0$ in Q and if there exist smooth simple arcs $\gamma(u)$, with $\gamma(0) = Q$, such that $lim_{u\to 0}(F_h(\gamma(u)))$ is finite. The set of all such finite values, obtained by taking different arcs $\gamma(u)$ through Q is the prefocal set δ_Q.

Let us consider first the point B, we obtain the following result :

Corollary 1.
For $h \neq 0$ and $h \neq 1$, let us consider the arc $\gamma(u)$ given by $u = x - (h+1)/h$ and $y = u^n$, n integer, $n > 0$, then
(i) $\gamma(0) = B$,
(ii) when $n = 1$, $lim_{u\to 0}(F_h(\gamma(u))) \in D_2'$,
(iii) when $n > 1$, $lim_{u\to 0}(F_h(\gamma(u))) \in D_0$.

Proof. Obviously, $\gamma(0) = B$. From (16), it is easy to check that :

- when $n = 1$, $lim_{u\to 0}(F_h(\gamma(u))) = (\frac{-(h+1)^2}{h^2}, \frac{h^2+1}{h^2})$,
  so, as the equation of D_2' in the plane (u, y) is $y = 2 - \frac{1-h}{1+h}u$,
  the point $(\frac{-(h+1)^2}{h^2}, \frac{h^2+1}{h^2})$ belongs to D_2'.
- when $n > 1$, $lim_{u\to 0}(F_h(\gamma(u))) = (\frac{2(h+1)}{1-h}, 0)$, which belongs to the line D_0.

□

Similar results can be proved regarding the points B' with lines D_2 and D_0, C with lines D_1' and D_0' and C' with lines D_1 and D_0'. From

the corollary regarding the point B and complementary calculations for the other points, we can write the following proposition and conjecture :

Proposition 3.
For $h \neq 0$ and $h \neq 1$,
(i) B and C are focal points of F_h,
(ii) B' and C' are focal points of F_h^{-1}.

Proof. (i) for point B comes from Corollary 3.1, $lim_{u\to 0}(F_h(\gamma(u)))$ has finite values for some arcs (here $\gamma(u) = (u, u^n)$), so B is a focal point and the set of finite values gives the prefocal set of B. It is not possible to calculate all values for all kind of arcs, anyway, as we obtain points of the two lines D_0 and D_2', we can conjecture that these two lines constitute the prefocal set of B. Similar results are obtained for C, B', and C', so we have the following conjecture: □

Conjecture
For $h \neq 0$ and $h \neq 1$, the prefocal sets of the focal points are :

$$\delta_B = D_0 \cup D_2', \delta_C = D_0' \cup D_1', \delta_{B'} = D_0 \cup D_2, \delta_{C'} = D_0' \cup D_1. \tag{26}$$

The following proposition permits to reinforce the conjecture.

Proposition 4.
For $h \neq 0$ and $h \neq 1$,
(i) The inverse image by F_h of the line D_2' minus the point C', $F_{-h}(D_2' \setminus \{C'\})$, is the focal point B, which is also a knot point of F_h^{-1}.
(ii) The inverse image by F_h of the line D_1' minus the point B', $F_{-h}(D_1' \setminus \{B'\})$, is the focal point C, which is also a knot point of F_h^{-1}.
(iii) The image by F_h of the line D_1 minus the point B, $F_h(D_1 \setminus \{B\})$, is the focal point C', which is also a knot point of F_h.
(iv) The image by F_h of the line D_2 minus the point C, $F_h(D_2 \setminus \{C\})$, is the focal point B', which is also a knot point of F_h.

Proof. Let $F_{-h}(D_2') = \{(x', y') \mid N_2'(x, y) = 0\}$. By definition we obtain $y' = 0$, so that: $F_{-h}(D_2') = \{(x', 0) \mid N_2'(x, y) = 0\}$. In other words, the coordinate x' is

$$x' = \frac{xN_1'(x,y)}{\Delta'(x,y)} \mid N_2'(x,y) = 0. \tag{27}$$

First of all, this displays:

$$N_1'(x,y) \mid (N_2'(x,y)=0) = (1-h)^2 + (1+h)^2, \tag{28}$$

furthermore, when $(x,y) \neq (0, 1+\frac{1}{h})$:

$$\Delta'(x,y) = h(1-h)[\frac{1+h}{h} + \frac{1+h}{1-h}x - y], \tag{29}$$

$$\Delta'(x,y) \mid (N_2'(x,y)=0) = h(1-h)[\frac{1+h}{1-h} + \frac{1-h}{1+h}]x, \tag{30}$$

and finally:

$$x' = \frac{(1-h)^2 + (1+h)^2}{h(1-h)[\frac{1+h}{1-h} + \frac{1-h}{1+h}]} = \frac{h+1}{h}, \tag{31}$$

so, $(x',0) = B$.

This proves also that the point B is a knot point for the map F_h^{-1}, as the image of a line by F_h^{-1}.

The proofs that $F_{-h}(D_1' \setminus \{B'\})$ is the point C, $F_h(D_1 \setminus \{B\})$ is the point C' and $F_h(D_2 \setminus \{C\})$ is the point B' are quite similar.

□

Remark. *The case $h = 1$ is considered in next section. When $h = 0$, $F_h = Id$ and the focal points are rejected to infinity.*

So, as it is mentionned in [Bischi *et al.*(1999), Gardini *et al.(2000)*] regarding invertible maps, D_2', which is focalized on B, should be a part of the prefocal set of B for F_h, as well as D_0, which is invariant by F_h and contains the point B. Moreover, as $F_h^{-1}(D_2' \setminus \{C'\})$ is reduced to a single point, the map F_h^{-1} cannot be locally invertible in the points of D_2' and its jacobian in each point of D_2' cancels. That property has been checked by using the software Maple.

We get equivalent properties for the points B' and C' by reversing the role of F_h^{-1} and F_h. Properties are detailed in Tables 1-2.

The Figure 1 shows the focal/knot points and the prefocal lines in the plane(x,y).

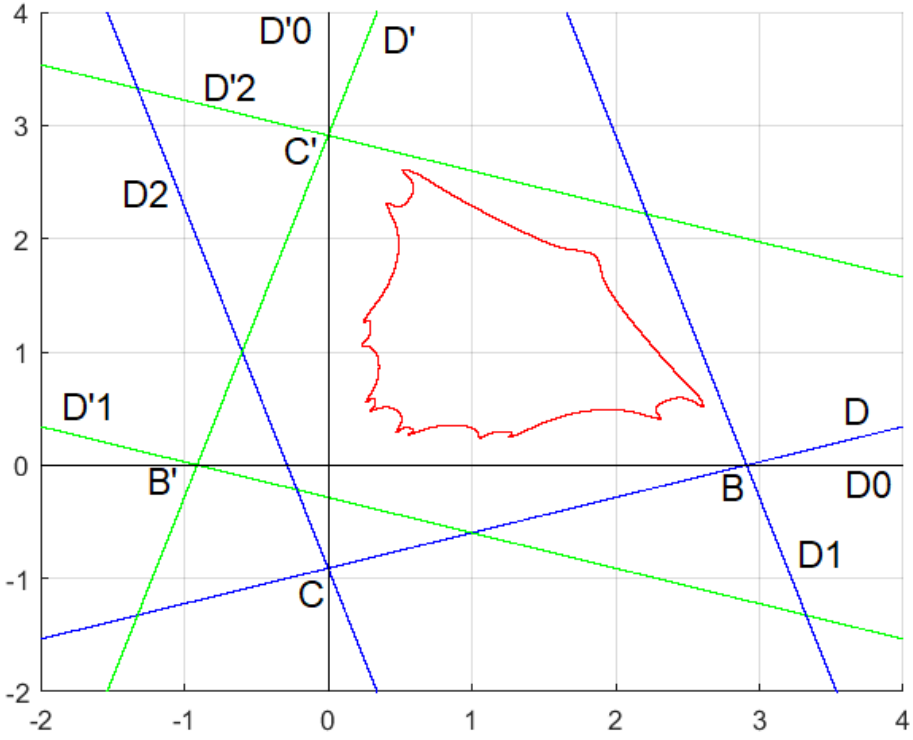

FIGURE 1. The focal/knot points and the corresponding prefocal lines are shown for $h = 0.5234$, an oval obtained for the initial condition (1,0.328) is plotted.

F_h		
focal points	B	C
knot points	B'	C'
prefocal sets	$D_0 \cup D_2'$	$D_0' \cup D_1'$
non definition set	D	
Property	$F_h^{-1}(D_2' \setminus \{C'\}) = B$	$F_h^{-1}(D_1' \setminus \{B'\}) = C$
Asymptotic focal set	$\left\{ \lim_{k\to+\infty} (F_h^{-n_k}(x))_{x\in I, I\subset D} \right\}$ when bounded	
Asymptotic prefocal set		$\left\{ \lim_{k\to+\infty} (F_h^{n_k}(x))_{x\in I, I\subset D_1'} \right\}$ $\left\{ \lim_{k\to+\infty} (F_h^{n_k}(x))_{x\in I, I\subset D_2'} \right\}$ when bounded

TABLE 1. Summary table of the particular sets of F_h.

F_h^{-1}		
focal points	B'	C'
knot points	B	C
prefocal sets	$D_0 \cup D_2$	$D_0' \cup D_1$
non definition set	D'	
Property	$F_h(D_2 \setminus \{C\}) = B'$	$F_h(D_1 \setminus \{B\}) = C'$
Asymptotic focal set	$\left\{ \lim_{k\to+\infty} (F_h^{n_k}(x))_{x\in I, I\subset D'} \right\}$ when bounded	
Asymptotic prefocal set		$\left\{ \lim_{k\to+\infty} (F_h^{-n_k}(x))_{x\in I, I\subset D_1} \right\}$ $\left\{ \lim_{k\to+\infty} (F_h^{-n_k}(x))_{x\in I, I\subset D_2} \right\}$ when bounded

TABLE 2. Summary table of the particular sets of F_h^{-1}.

2.4. **Asymptotic prefocal and focal sets.** Considering the map F_h, we introduce the following definitions :

Definition 1. *We call asymptotic focal set (AFS) the set of bounded limits of the preimages by F_h of points from a bounded subset I of the non-definition set D of F_h, that means $\left\{ \lim_{k\to+\infty} (F_h^{-n_k}(x))_{x\in I, I\subset D} \right\}$, if this set exists.*

Definition 2. *We call asymptotic prefocal set (APS) the set of bounded limits of the iterates by F_h of points from a bounded subset I of the prefocal set S of F_h, that means* $\left\{\lim_{k\to+\infty}(F_h^{n_k}(x))_{x\in I, I\subset S}\right\}$, *if this set exists.*

It is important to denote that such limits have not always finite values, due to the possible existence of divergent orbits. Let us remark that equivalent definitions can be introduced for $F_h^{-1} = F_{-h}$. The corresponding definitions are given in Tables 1-2. Those definitions are illustrated in the paragraph devoted to numerical simulations.

2.5. **Theorem of Sanz-Serna and sympletic birational transformation of the plane.** First, we include some results on the fixed points of this mapping.

Proposition 5. *The fixed points of F_h are $(0,0)$, $(1,1)$. The point $(0,0)$ is a saddle. The linearized map at the point $(1,1)$ is a rotation.*

Proof. The list of fixed points can be easily found by direct analysis of the equations $F_h(x,y) = (x,y)$ and it coincides with the zeros of $f(x,y)$. In the case of the Lotka-Volterra system, this yields to $(x,y) = (0,0)$ and $(x,y) = (1,1)$. To study the nature of the fixed points, it is quite convenient to use the equation (after changing h into $2h$) :

$$(I - hDf(z))A = (I + hDf(z')). \tag{32}$$

In case of a fixed point $z' = z = z_0$, this yields:

$$\det(A - \lambda I) = \det([I - hDf(z_0)]^{-1}[I + hDf(z_0)] - \lambda(I - hDf(z_0))]), \tag{33}$$

so that the eigenvalues λ of the jacobian matrix of F_h at a fixed point are solutions of

$$\det[(1-\lambda)I + (1+\lambda)hDf(z_0)] = 0. \tag{34}$$

For the Lotka-Volterra case, from equations (1) and (13), it comes:

$$Df(z_0) = \begin{pmatrix} 1 - y_0 & -x_0 \\ y_0 & x_0 - 1 \end{pmatrix}, \tag{35}$$

So, in the case $(x_0, y_0) = (0,0)$, this yields:

$$\lambda = \lambda_1 = \frac{1+h}{h-1}, \lambda = \lambda_2 = \frac{1-h}{1+h}, \tag{36}$$

hence the two eigenvalues satisfy $\mid \lambda_1 \mid\mid \lambda_2 \mid = 1$. If $h \neq 1$, the point $(0,0)$ is a saddle.

Let us consider now the case $(x_0, y_0) = (1,1)$. Then this yields:

$$\lambda = \lambda_1 = \frac{1+\mathrm{ih}}{1-\mathrm{ih}}, \lambda = \lambda_2 = \overline{\lambda_1} = \frac{1-\mathrm{ih}}{1+\mathrm{ih}}, \tag{37}$$

$$\mid \lambda_1 \mid = \mid \lambda_2 \mid = 1, \tag{38}$$

so that:

$$\lambda_1 = \exp(\mathrm{i}\theta), \lambda_2 = \exp(-\mathrm{i}\theta), \tag{39}$$

so the linearized map at the point $(x_0, y_0) = (1,1)$ is a rotation.

□

We include a proof of the theorem of Sanz-Serna:

Theorem 6. *The KHK map of the Lotka-Volterra system preserves the (singular) volume form:*

$$\Omega = \frac{dx \wedge dy}{xy}. \tag{40}$$

Proof. Consider

$$\Delta := \Delta(x, y, h) = 1 - h^2 - h(1-h)x + h(1+h)y, \tag{41}$$

and change in Δ, both (x, y) into (x', y') and h into $-h$. This yields

$$\Delta' := \Delta(x', y', -h) = 1 - h^2 + h(1+h)x' - h(1-h)y'. \tag{42}$$

Next compute directly the differentials and obtain:

$$\frac{dx \wedge dy}{\Delta} = \frac{dx' \wedge dy'}{\Delta'}. \tag{43}$$

Now from (16), it follows:

$$(\frac{x'}{x} + \frac{y'}{y})\Delta = (1+h)^2 + (1-h)^2 = 2(1+h^2). \tag{44}$$

By the same transformation, we obtain:

$$(\frac{x'}{x} + \frac{y'}{y})\Delta = (\frac{x}{x'} + \frac{y}{y'})\Delta', \tag{45}$$

and this yields:

$$\frac{dx \wedge dy}{xy} = \frac{dx' \wedge dy'}{x'y'}. \tag{46}$$

□

The set of birational transformations of the plane which preserves the volume form $\frac{dx \wedge dy}{xy}$ is more shortly called "symplectic birational transformations of the plane" in the litterature. For instance, this is the terminology used in the article [Blanc (2003)]. In this article the author proves the following remarkable result which looks in particular useful for further studies of discretized Lotka-Volterra of the plane (indeed, theorem 2 proves that the map F_h belongs to that set) :

Proposition 7. *The group of symplectic birational transformations of the plane is generated by the group of 2x2 matrices with determinant equal to 1, $SL(2,\mathbb{Z})$, the torus $\mathbb{C}^{*2}$ and a special map of order 5: $P : (x,y) - - > (y,(y+1)/x)$.*

The mapping P is a special case of the so-called Lyness map ([Duistermaat(2010), Gálvez-Carrillo & Mañosa(2015), Gardini *et al.(2000)*]).

2.6. **Integrability of the discretized Lotka-Volterra in the case $h = 1$.** In this section we focus in the special case where the parameter $h = 1$. Replacing $h = 1$ in the formula (16) yields to the map:

$$\Delta := 2y, \tag{47}$$

$$\begin{aligned} x' &= \frac{x}{y}(2-x) \\ y' &= \frac{y}{y}(x) = x. \end{aligned} \tag{48}$$

Moreover, the inverse map is given by :

$$\begin{aligned} x' &= y \\ y' &= \frac{y(2-y)}{x}. \end{aligned} \tag{49}$$

It is easy to see that as h tends to 1, C is merging with the origin and $B = (2,0)$. The focal points of the inverse map are $B' = (0,0)$ and $C' = (0,2)$. A direct calculus allows to check that Proposition 2 remains true for $h = 1$. We obtain :

$$D_1 : x = 2, D_2 : x = 0, D_1' : y = 0, D_2' : y = 2, \tag{50}$$

$$F_h^{-1}(D_2' \setminus \{C'\}) = B, F_h^{-1}(D_1' \setminus \{B'\}) = C, \tag{51}$$

$$F_h(D_2 \setminus \{C\}) = B', F_h(D_1 \setminus \{B\}) = C'. \tag{52}$$

We consider then

$$x' + y' - 2 = \frac{(x-y)(2-x)}{y}, \tag{53}$$

$$x' - y' = \frac{x(2-x-y)}{y}, \tag{54}$$

$$\frac{(x'+y'-2)(x'-y')}{x'y'} = -\frac{(x+y-2)(x-y)}{xy}, \tag{55}$$

so that we deduce that the mapping preserves the pencil of conics:

$$[(x+y-2)(x-y)]^2 = \mu[xy]^2. \tag{56}$$

Figure 2 shows the pencil of conics for $\mu = \alpha^2$, α varying from -2 to 2 with step 0.05.

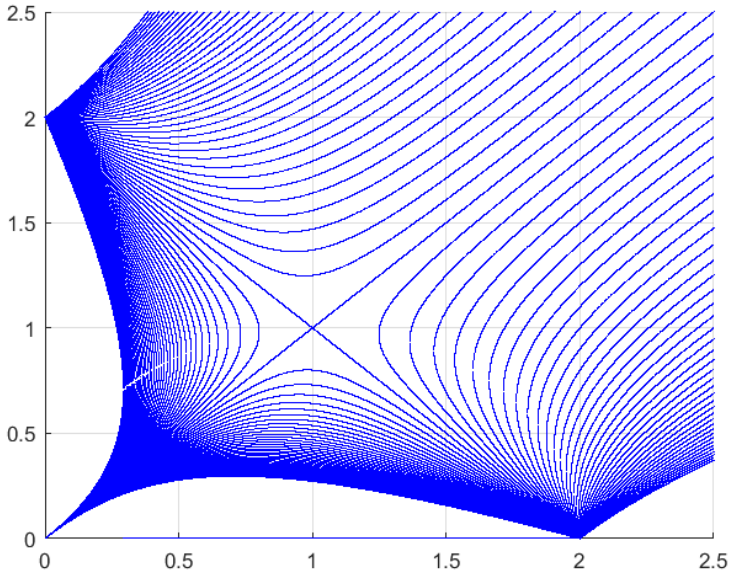

FIGURE 2. The pencil of conics

Furthermore, existence of cycles of order 4 can be shown in the case $h = 1$:

Proposition 8. *For all x real, $x \neq 0$, the points $(x, x), (2-x, x), (2-x, 2-x), (x, 2-x)$ form a cycle of order 4.*

This can be easily checked by direct computation. Moreover, there are numerical evidences that the map is not periodic of period 4, that means that $F^4_{h=1} \neq F_{h=1}$. Indeed, some orbits turn successively around the fixed point $A(1, 1)$ and go towards infinity. For instance, the initial conditions chosen in Figure 3 give rise to orbits that go towards infinity asymptotically to the lines $y = 2 - x$ or $y = x$.

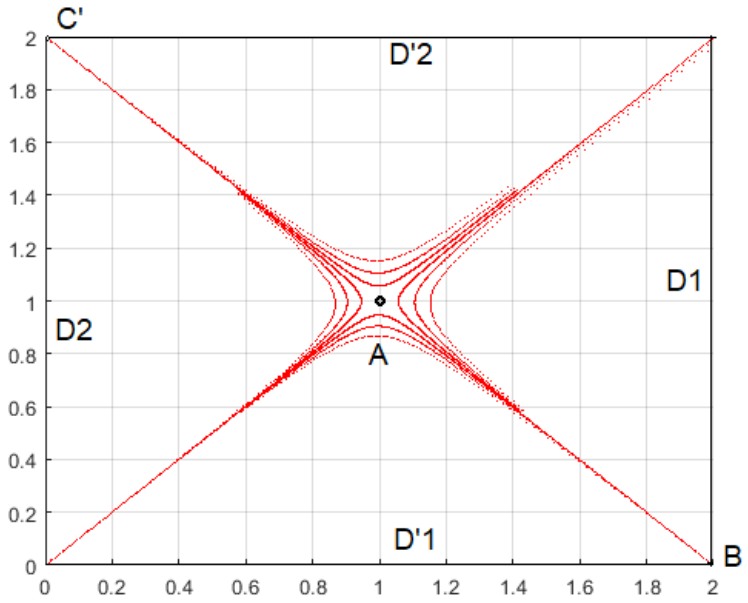

FIGURE 3. Three orbits obtained numerically for $h = 1$, initial conditions are (0.58,1.4), (0.58,1.41), (0.58,1.417). D_2 and D'_1 are merged with the axis $x = 0$ and $y = 0$.

3. Numerical simulations and basin boundaries in the case $0 < h < 1$

Numerical simulations in the case $0 < h < 1$ are proposed in Figures 4-14. All figures have been plotted using Matlab (Figures 1 - 8) or a Fortran specific software (Figures 9 - 14).

In the plane(x, y), some orbits are ovals, that means invariant closed curves, or order k cyclic ovals, that means k invariant closed curves

whose points exchange cyclically, one on each of the k curves. An oval or an order k cyclic oval is an invariant set by F_h.

In Figure 4, h is small and the plotted ovals around the center fixed point $A(1,1)$ look very similar to the trajectories of the Lotka-Volterra system. When h increases between 0 and 1 (see Figures 5-14), the ovals change their shape and some of them are cyclic. For instance, in Figure 6, an order 20 cyclic oval is obtained and in Figure 7, an order 55 cyclic oval and an order 9 cyclic one are obtained from different initial conditions.

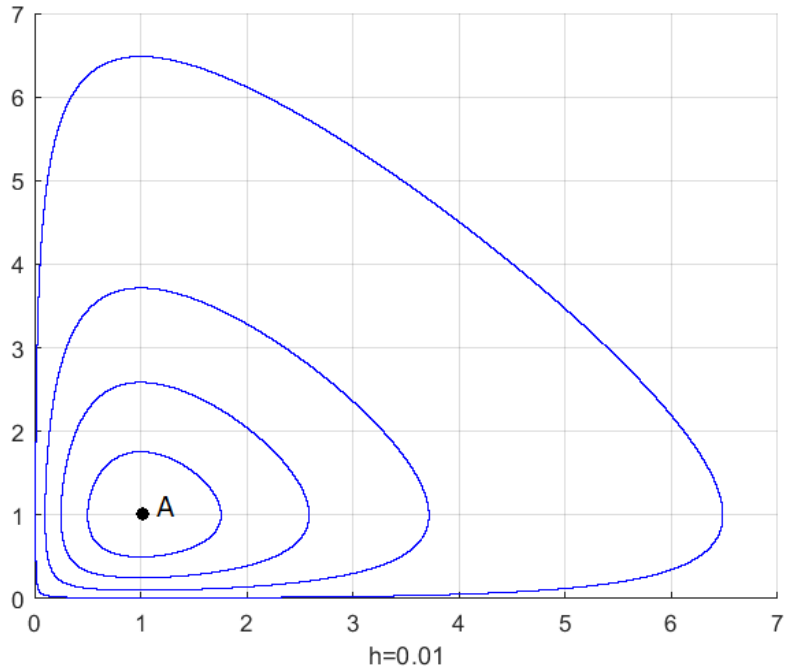

FIGURE 4. h=0.01, ovals obtained with 4 different initial conditions (1,0.01), (1,0.1), (1,0.25), (1,0.5)

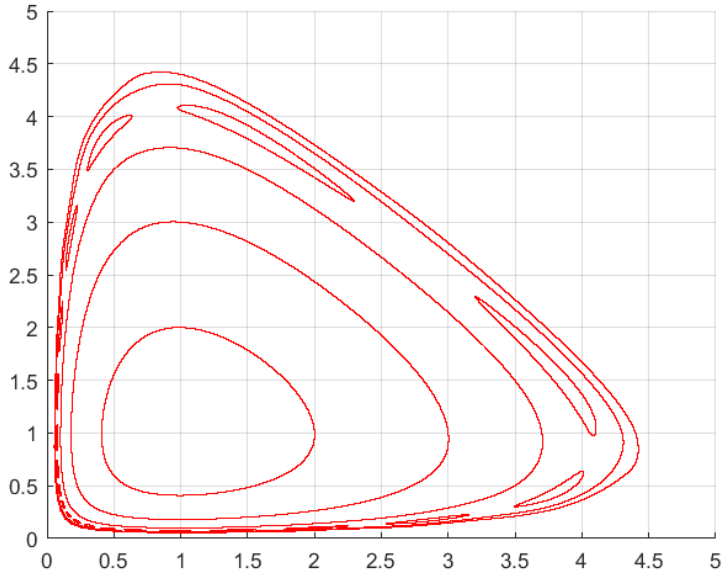

FIGURE 5. h=0.2, invariant curves or ovals obtained with 6 different initial conditions (1,2), (1,3), (1,3.7), (1,4.1), (1, 4.3), (1,4.4)

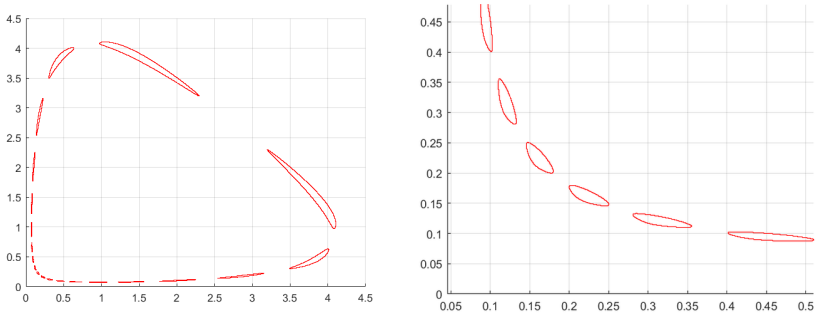

FIGURE 6. h=0.2, focus on the order 20 cyclic oval obtained with the initial condition (1,4.1). The Figure on the right shows a magnification in the square $[0, 0.5]^2$.

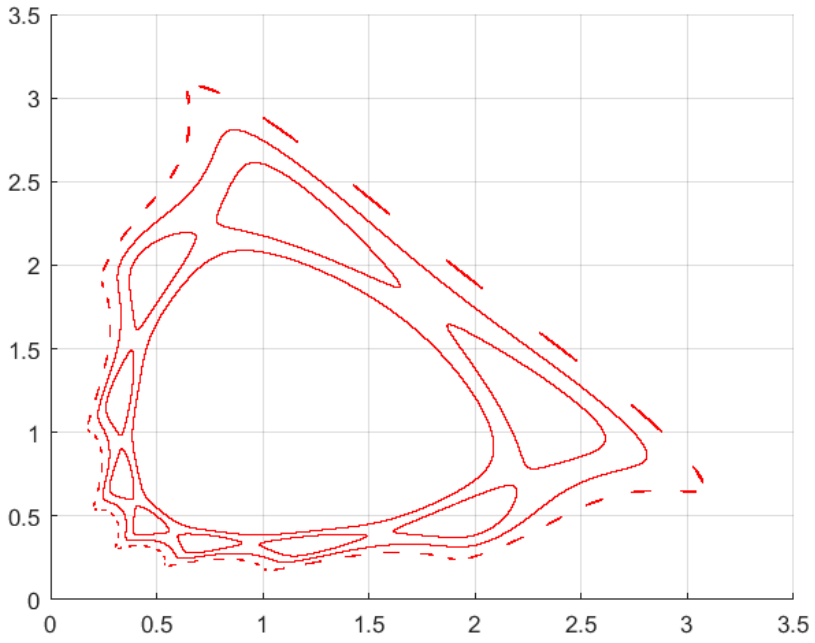

FIGURE 7. h=0.38, ovals obtained with 4 different initial conditions (0.55,0.5), (0.5,0.5), (0.5,0.35), (0.5,0.3). (0.5,0.3) gives rise to an order 55 cyclic oval and (0.5,0.5) gives rise to an order 9 cyclic oval.

We can define the basin of ovals as the set of initial conditions giving rise to an oval or a cyclic oval.

Figure 9 shows the basin of initial conditions giving rise to ovals. The basin has been obtained using numerical simulations : each pixel corresponds to an initial condition and is plotted in beige when the orbit remains bounded after N iterations (in Figure 9, $N = 10000$). Its shape looks "like a bat", as the larger oval obtained Figure 8 with the initial condition $(1, 0.328)$. The initial conditions taken outside this basin give rise to unbounded trajectories in the plane (x, y). This basin corresponds to the domain of stability of the map (16) in the sense of Lagrange. We remark that the basin is located in the first quadrant inside the area limited by the straight lines D_1, D_2', D_0 and D_0'. Let us recall that D_2' and D_0 are the prefocal set of the focal point B for F_h and D_1 and D_0' are the prefocal set of the point C' for F_h^{-1}. D_1 and D_2' are symmetrical each other with respect to the first bisector.

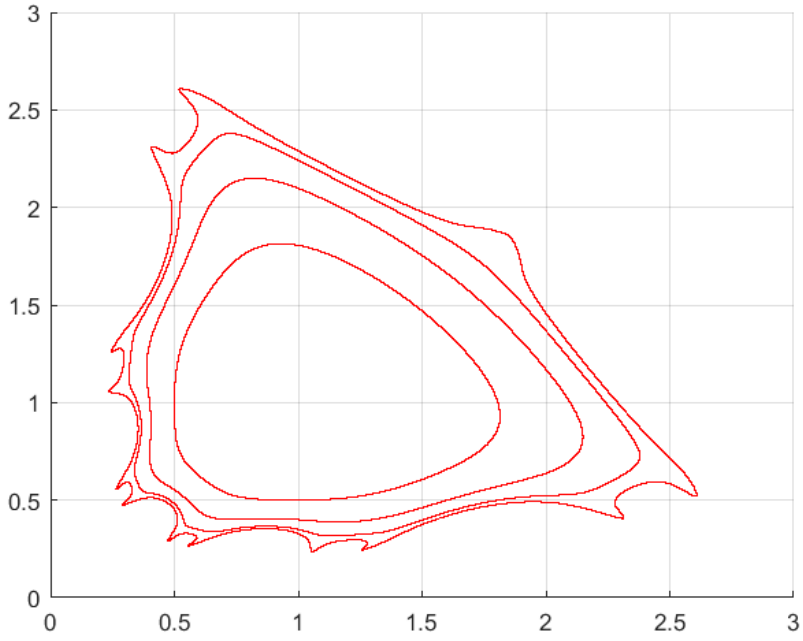

FIGURE 8. h=0.5234, ovals obtained with 4 different initial conditions (1,0.5), (1,0.4), (1,0.35), (1,0.328). The oval obtained with the initial condition (1,0.328) seems to be very close to the boundary of the basin (cf. Figure 9).

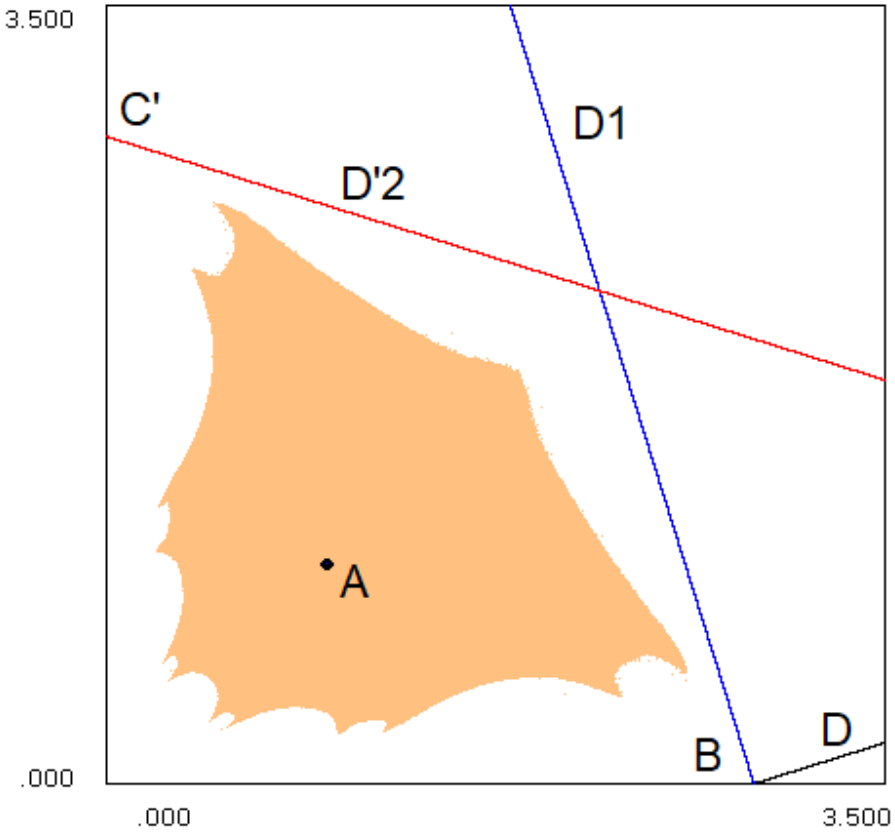

FIGURE 9. h=0.5234, the basin of ovals has "the shape of a bat". The lines D, D_2' and D_1, the point $A(1,1)$ and the focal points B and C' are plotted. The basin is located inside the area limited by the lines D_1 and D_2' and the two axis $x = 0$ and $y = 0$.

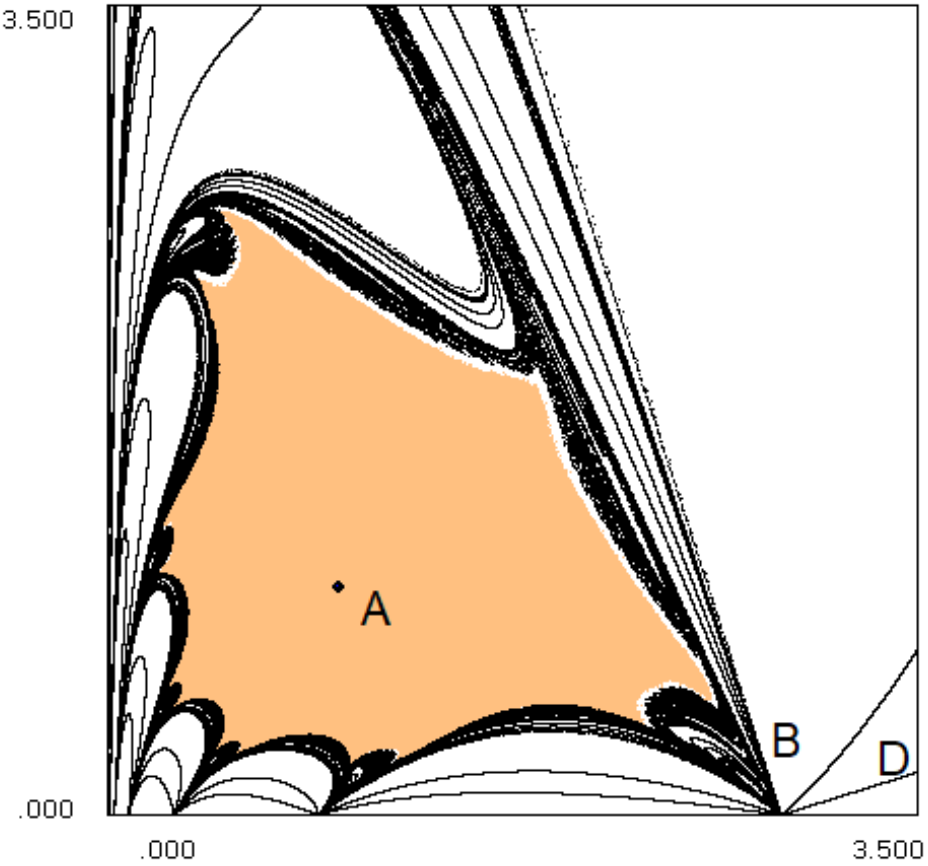

FIGURE 10. h=0.5234, 250 preimages of points of the line D, taken in the interval $[-10, 10]$ with a step of 10^{-5}, are plotted in black. These points are a part of the asymptotic focal set (AFS), as defined in Definition 1. The role of B as a knot for the map F_h^{-1} appears: infinitely many curves of preimages of points of D are issuing from B.

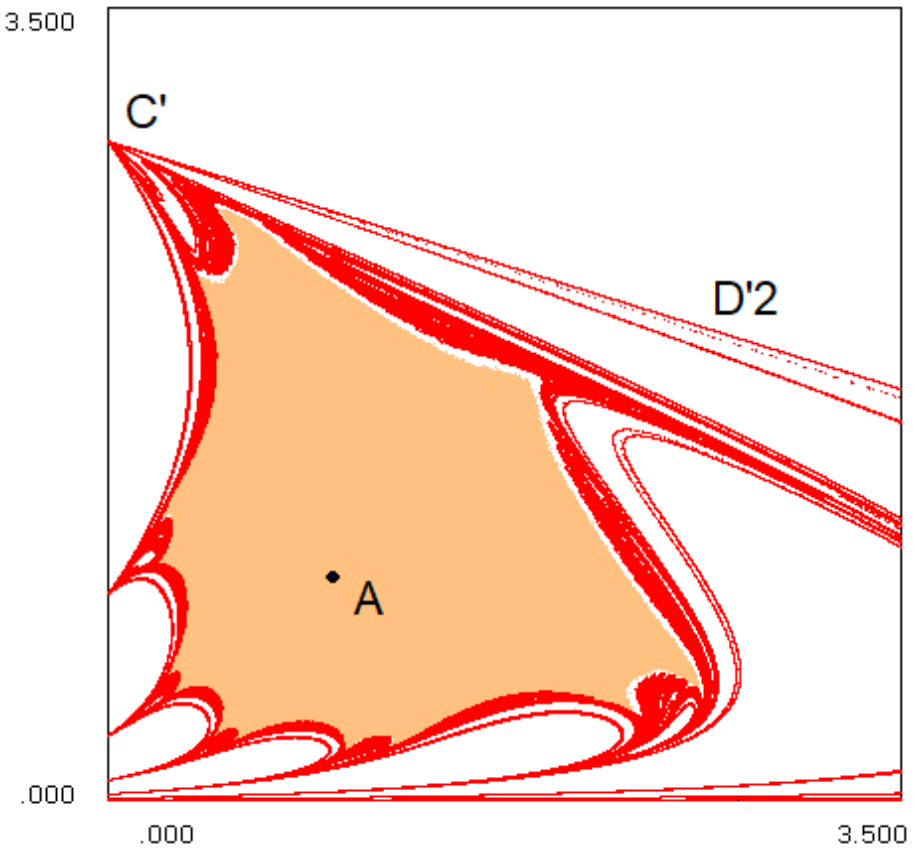

FIGURE 11. h=0.5234, 250 images of points of the prefocal line D'_2, taken in the interval $[-10, 10]$ with a step of 10^{-5}, are plotted in red. These points form part of the asymptotic prefocal set (APS), as defined in Definition 2. The role of C' as a knot for the map F_h appears: infinitely many curves of images of points of D'_2 are issuing from C'.

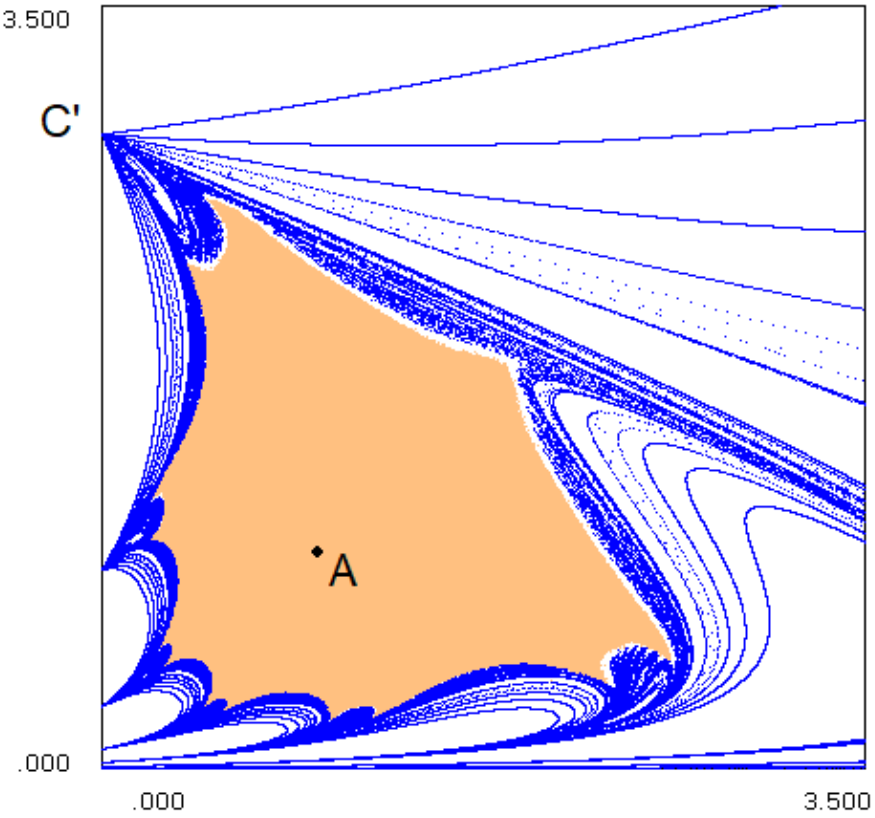

FIGURE 12. h=0.5234, 250 images of points of the prefocal line D_1', taken in the interval $[-10, 10]$ with a step of 10^{-5}, are plotted in blue. These points form part of the asymptotic prefocal set (APS), as defined in Definition 2. D_1' is fully located outside of the first quadrant, so is not plotted on the Figure. C' is a knot point for F_h.

In Figures 10-12, we have plotted 250 preimages of points of the line D and 250 images of points of the prefocal lines D_1' and D_2', these points respectively form part of the asymptotic focal set (AFS) and the asymptotic prefocal set (APS). It is easy to see that some of these points accumulate along the boundary of the basin of ovals. This property can be observed for one dimensional maps and also for some two-dimensional maps [Bischi *et al.*(1999), Gardini *et al.(1999)*]. Let us remark that the preimages of points of D_1 and D_2 are symmetrical to images of points of D_1 and D_2, due to the property of the inverse $F_h^{-1} = F_{-h}$. Some of these points also accumulate along the boundary.

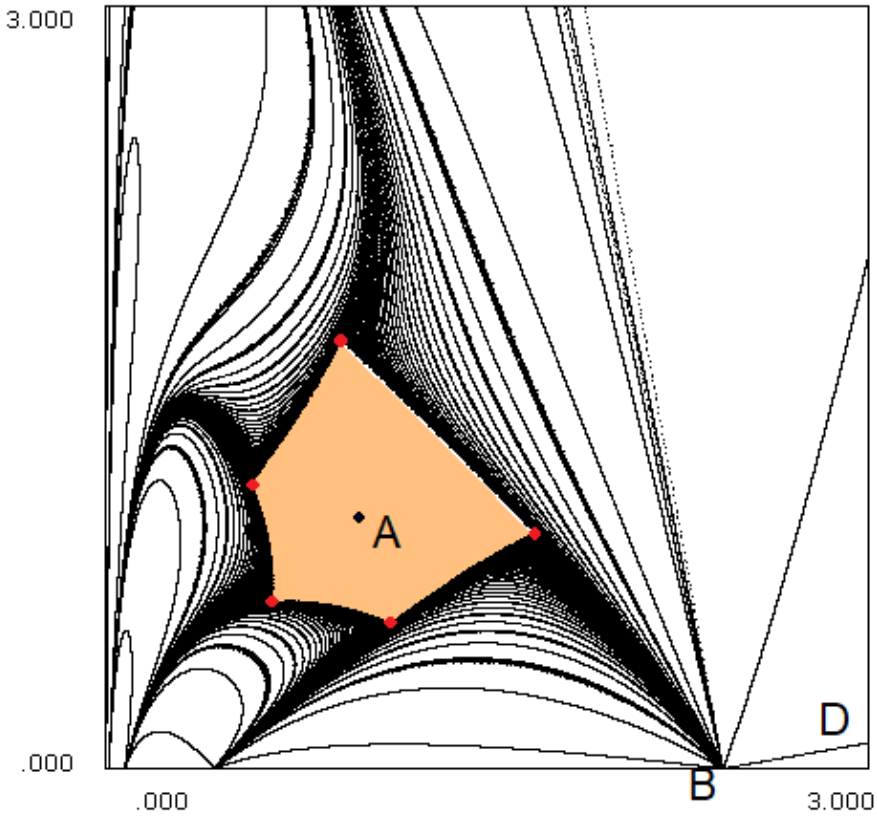

FIGURE 13. h=0.7, 250 preimages of points of the line D, taken in the interval $[-10, 10]$ with a step of 10^{-5}, are plotted. These points form part of the asymptotic focal set (AFS), as defined in Definition 1. An order 5 saddle cycle (points in red) is obtained close to the boundary of the basin.

So subsets of the (AFS) and (APS) sets permit to obtain the shape of the boundary of the stable domain in the sense of Lagrange.

The same property is obtained for different values of h. See Figures 13-14 for $h = 0.7$ and $h = 0.9$. Preimages of points of D have only been plotted.

It is important to denote that these points do not give the boundary, they are converging towards it. Indeed, the boundary separates the basin of initial conditions giving rise to bounded trajectories from the set of initial conditions giving rise to divergent trajectories going to infinity. So, this boundary is a repelling set for some orbits of F_h and

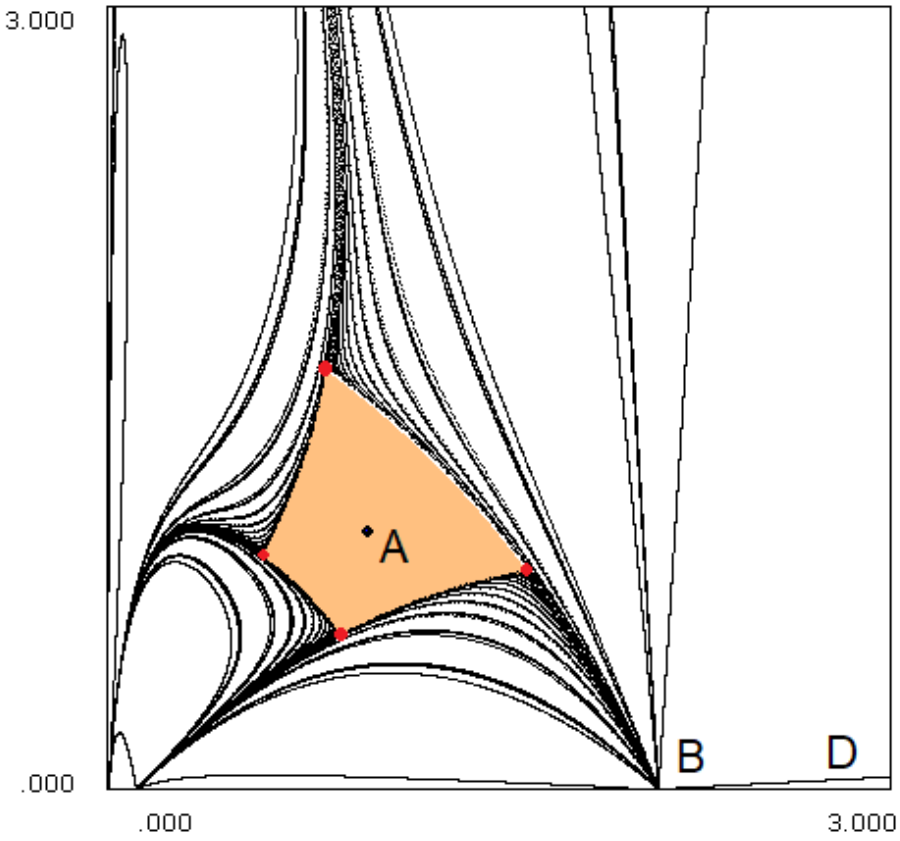

FIGURE 14. h=0.9, 100 preimages of points of the line D, taken in the interval $[-10, 10]$ with a step of 10^{-5}, are plotted. These points form part of the asymptotic focal set (AFS), as defined in Definition 1. An order 4 saddle cycle (points in red) is obtained close to the boundary of the basin.

an attracting set for some orbits of the inverse map F_h^{-1}. Anyway, the AFS and APS sets permit to obtain the shape of this boundary.

Usually, the boundary of basins is related to the existence of saddle points, indeed, attractive invariant manifolds of saddle points are parts of the basin boundary. For the value of $h = 0.5234$, we have not found order k saddle points close to the boundary with an order less than 20, but for $h = 0.7$, we have found an order 5 saddle cycle (see Figure 13) and for $h = 0.9$, an order 4 saddle cycle (see Figure 14).

Their attractive invariant manifolds are probably part of the boundary of the basin of ovals.

The Figures 10-14 permit also to put in evidence the role of knot points B for F_h^{-1} and C' for F_h. Infinitely many curves respectively images of specific lines by F_h^{-1} or F_h are issuing from these points.

Moreover, we can remark that the size of the basin of ovals decreases when h increases from 0 to 1.

4. Conclusion and perspectives

This article revisits a discretization of quadratic vector fields called the Kahan-Hirota-Kimura discrete dynamical systems (KHK map). The study of this map relates with integrable systems and soliton theory, in particular with QRT-maps ([Celledoni *et al.*(2015), Celledoni *et al.*(2014), Celledoni *et al.*(2013), Duistermaat(2010), Francoise & Ragnisco(1999), Gálvez-Carrillo & Mañosa(2015), Van der Kamp *et al.(2021)*, Quispel *et al.(1988)*, Quispel *et al.(1989)*, Petrera *et al.(2019)*]). The proof of the Jacobian identity is included in the article. We focus on the discretization of the classical Lotka-Volterra prey-predator system and we derive a direct proof of the Sanz-Serna theorem from the Jacobian identity. The discretization gives rise to a birational map with denominator that can cancel. Such map can be studied by using specific tools as focal points, prefocal sets and knot points that are involved in the dynamics. Several numerical simulations are further discussed. They give evidences that for some values of the parameter, the boundary of the domain of Lagrange stability displays an interesting geometric structure and the "shape of a bat". Moreover, we have defined asymptotic prefocal and asymptotic focal sets, whose subsets permit to obtain the shape of the boundary by another way.

5. Acknowledgments

JPF thanks Pr. Daisuke Tarama for his kind invitation to give a talk at the workshop "Geometric Structures and Differential Equations - Symmetry, Singularity, and Quantization -". This talk initiated this joint article with DFP. The authors thank the reviewers for their valuable comments, which greatly contributed to the improvment of the paper.

References

[Bischi *et al.*(1999)] Bischi, G. I.; Gardini, L.; Mira, C. *Plane maps with denominator. I: some generic properties.* Int. J. Bifurc. Chaos Appl. Sci. Eng., vol 9, n° 1 (1999), 119-153.

[Bischi *et al.*(2003)] Bischi, G. I.; Gardini, L.; Mira, C. *Plane maps with denominator. II. Noninvertible maps with simple focal points.* Int. J. Bifurc. Chaos Appl. Sci. Eng., 13 (2003), no. 8, 2253–2277.

[Bischi *et al.*(2005)] Bischi, G. I.; Gardini, L.; Mira, C. *Plane maps with denominator. III. Nonsimple focal points and related bifurcations.* Int. J. Bifurc. Chaos Appl. Sci. Eng., 15 (2005), no. 2, 451–496.

[Bischi *et al.*(2011)] Bischi, G. I.; Gardini, L.; Mira, C. *Contact bifurcations related to critical sets and focal points in iterated maps of the plane.* Proc. Intern. Workshop Future Directions in Difference Equations, 2011, 15-50.

[Blanc (2003)] Blanc, J. *Symplectic birational transformations of the plane.* Osaka J. Math. 50 (2013), no. 2, 573–590.

[Celledoni *et al.*(2013)] Celledoni, E.; McLachlan, R. I.; Owren, B.; Quispel, G. R. W. *Geometric properties of Kahan's method.* J. Phys. A 46 (2013), no. 2, 025201, 12 pp.

[Celledoni *et al.*(2014)] Celledoni, E.; McLachlan, Robert I.; McLaren, D. I.; Owren, B.; Quispel, G. R. W. *Integrability properties of Kahan's method.* J. Phys. A 47 (2014), no. 36, 365202, 20 pp.

[Celledoni *et al.*(2015)] Celledoni, E.; McLachlan, R. I.; McLaren, D. I.; Owren, B.; Quispel, G.R.W. *Discretization of polynomial vector fields by polarization.* Proc. A. 471 (2015), no. 2184, 20150390, 10 pp.

[Duistermaat(2010)] Duistermaat, J. *Discrete integrable systems. QRT maps and elliptic surfaces.* Springer Monographs in Mathematics. Springer, New York, 2010. xxii+627 pp.

[Francoise & Ragnisco(1999)] Francoise, J. P.; Ragnisco, O. *An iterative process on quartics and integrable symplectic maps.* Symmetries and integrability of difference equations (Canterbury, 1996), 56–63, London Math. Soc. Lecture Note Ser., 255, Cambridge Univ. Press, Cambridge, 1999.

[Francoise & Fournier-Prunaret(2023)] Francoise, J. P.; Fournier-Prunaret, D. *Discretization of the Lotka-Volterra System.* To appear in RIMS Kôkyûroku, 2023.

[Gardini *et al.(1999)]* Gardini, L.; Bischi, G.I.; Fournier-Prunaret, D. *Basin boundaries and focal points in a map coming from Bairstow's method.* Chaos 9 (1999), no. 2, 367–380.

[Gardini *et al.(2000)]* Gardini, L.; Bischi, G. I.; Mira, C. *Invariant curves and focal points in a Lyness iterative process.* Dynamical systems and functional equations (Murcia, 2000). Int. J. Bifurc. Chaos Appl. Sci. Eng., 13 (2003), no. 7, 1841–1852.

[Gálvez-Carrillo & Mañosa(2015)] Gálvez-Carrillo, I.; Mañosa, V. *Periodic orbits of planar integrable birational maps.* Nonlinear maps and their applications, 13–36, Springer Proc. Math. Stat., 112, Springer, Cham, 2015.

[Hirota & Kimura(2000)] Hirota, R.; Kimura, K. *Discretization of the Euler top.* J. Phys. Soc. Japan 69 (2000), no. 3, 627–630.

[Kahan(1993)] Kahan W. *Unconventional numerical methods for trajectory calculations* Unpublished Lecture Notes (1993).

[Van der Kamp *et al.(2021)]* Van der Kamp, P. H.; McLaren, D. I.; Quispel, G. R. W. *Generalised Manin transformations and QRT maps.* J. Comput. Dyn. 8 (2021), no. 2, 183–211.

[Kimura & Hirota(2000)] Kimura, K.; Hirota, R. *Discretization of the Lagrange top.* J. Phys. Soc. Japan 69 (2000), no. 10, 3193–3199.

[Petrera *et al.(2009)]* Petrera M.; Pfaeller A.; Suris Y. *On integrability of Hirota-Kimura-Type Discretizations. Experimental Study of the discrete Clebsch System.* Experimental Mathematics, Vol. 18 (2009), N° 2.

[Petrera *et al.(2019)]* Petrera, M.; Smirin, J.; Suris, Y. *Geometry of the Kahan discretizations of planar quadratic Hamiltonian systems.* Proc. A. 475 (2019), no. 2223, 20180761, 13 pp.

[Quispel *et al.(1988)]* Quispel, G. R. W.; Roberts, J. A. G.; Thompson, C. *J. Integrable mappings and soliton equations.* Phys. Lett. A 126 (1988), no. 7, 419–421.

[Quispel *et al.(1989)]* Quispel, G. R. W.; Roberts, J. A. G.; Thompson, C. J. *Integrable mappings and soliton equations. II.* Phys. D 34 (1989), no. 1-2, 183–192.

[Ratiu(2006)] Ratiu T. *Nonabelian Semi-direct Product Orbits and Their Relation to Integrable Systems* Talk at the International Workshop "Geometric Integration" at the Mathematisches Forschunginstitut Oberwolfach. March 2006.

[Sanz-Serna(1994)] Sanz-Serna, J. M. *An unconventional symplectic integrator of W. Kahan.* A Festschrift to honor Professor Robert Vichnevetsky on his 65th birthday. Appl. Numer. Math. 16 (1994), no. 1-2, 245–250.

[Tramontana(2016)] Tramontana, F. *Maps with vanishing denominator explained through applications in Economics.* J. Phys. (2016) Conf. Ser. 692 012006, 12 pp.

Sorbonne-Université, Laboratoire Jacques–Louis Lions, UMR 7598 CNRS,, 4 Place Jussieu, 75252, Paris, France, Jean-Pierre.Francoise@sorbonne-universite.fr

Université de Toulouse, INSA Toulouse, 135 avenue de Rangueil, 31077, Toulouse cedex 04, France, daniele.fournier@insa-toulouse.fr